

Short-term Energy Recovery Control for Virtual Inertia Provision by Renewable Energy Sources

1st Juan Manuel Mauricio

Dept. of Electrical Engineering
Universidad de Sevilla
Sevilla, Spain
jmmauricio@us.es

2nd Kyriaki-Nefeli Malamaki

Dept. of Electrical & Computer Engineering
Aristotle University of Thessaloniki
Thessaloniki, Greece
kyriaki nefeli@hotmail.com

3rd José María Maza-Ortega

Department of Electrical Engineering
Universidad de Sevilla
Sevilla, Spain
jmmaza@us.es

4th Georgios C. Kryonidis

Dept. of Electrical & Computer Engineering
Aristotle University of Thessaloniki
Thessaloniki, Greece
kryonidi@auth.gr

5th Manuel Barragán-Villarejo

Dept. of Electrical Engineering
Universidad de Sevilla
Sevilla, Spain
manuelbarragan@us.es

6th Spyros I. Gkavanoudis

Dept. of Electrical & Computer Engineering
Aristotle University of Thessaloniki
Thessaloniki, Greece
s.gkavan@gmail.com

7th Charis S. Demoulias

Dept. of Electrical & Computer Engineering
Aristotle University of Thessaloniki
Thessaloniki, Greece
chdimoul@auth.gr

Abstract—The proliferation of Converter-Interfaced Renewable Energy Sources (CIRES), which are inertia-less, and the gradual decommissioning of synchronous generation have posed several challenges to the electric power system. This has motivated a complete a shift in the CIRES design and its corresponding control philosophy. Integrating Energy Storage Systems (ESS) within CIRES enables the implementation of different operating modes allowing them to provide ancillary services (AS) in a similar way to the synchronous generation. In order to tackle with those short-term response AS, such as virtual inertia, fast ESS (FESS) solutions with high power-to-energy ratio, particularly flywheels and supercapacitors, are preferred. In spite of several control algorithms have been proposed to provide such fast AS, very little research effort has been paid on the proper FESS energy recovery after the AS provision. This task is particularly challenging, since supercapacitors must be operated at a certain state of charge to guarantee that the required AS can be provided within its operational limits. This paper aims to fill this gap by proposing a new energy recovery control scheme for supercapacitors after the provision of short-term AS, such as virtual inertia. The proposed control is validated via simulations which clearly highlights its adequate performance.

Index Terms—renewable generation, ancillary services, energy storage systems, virtual inertia, voltage source converters, supercapacitors, renewable energy source.

I. INTRODUCTION

The advent of Renewable Energy Sources (RES) has introduced a new era for the electric power grids which rely more and more on power electronics. As a matter of fact, RES like photovoltaic (PV) and wind generation employ Voltage Source

Converters (VSCs) as their main interface with the grid. The ever-increasing penetration of this type of converter-interfaced RES (CIRES), characterised by an inertia-less nature and a current control mode, replacing synchronous generators jeopardizes the stability and robustness of the power grid. These issues could be tackled if the enhanced controllability of the VSCs is exploited and new control philosophies are adopted. In this way, CIRES may provide ancillary services (AS) in a manner similar to synchronous generators, e.g. reactive power capability, primary frequency regulation (PFR) through P - f droop control, virtual (synthetic) inertia, etc. [1]. In order to make the provision of the active power-related AS feasible without any active power curtailment, the integration of Energy Storage Systems (ESS) is inevitable. Different ESS technologies are available in the market but their specific application to provide a given AS must consider the power and energy requirements. Broadly speaking, AS with large duration and high energy requirements, such as PFR and demand-response, could be provided by battery ESS (BESS). Conversely, short-term AS involving high instantaneous power like virtual inertia mandate the use of fast ESS (FESS) technologies [2], e.g. flywheels (FWs) [3] and supercapacitors (SCs) [4].

There are plenty research studies for the proper control and the topology of the combined CIRES and ESS for the provision of active power-related AS, e.g. PFR [5]–[8], power-smoothing (also referred as ramp-rate limitation), [2], [9], [10], peak-shaving [11], etc. These strategies have been successfully applied to either wind [9], [11] or PV generation [2], [6], [10]. Although these studies include a State-Of-Charge (SoC) control after the AS provision, this control comes as a second

priority and limited results are presented, while they mostly focus on the proper CIRES control for the AS provision.

Furthermore, the types of ESS in these studies are usually electrochemical BESS [5], [6], [10] or Hybrid ESS (HESS), [7]–[9], [11], [12] which consist of a BESS and a FESS (either SC [7], [8], [11] or FW, [12]). Regarding the BESS, although there are many research studies for the proper SoC restoration, the involved dynamics are in the order of minutes (5-15). This is sufficient for low-frequency power smoothing or peak-shaving, but for other AS, e.g. PFR or even virtual inertia, the BESS reaction is too slow. Regarding the HESS, the main drawback of the aforementioned studies is that the FESS SoC is treated similarly to the BESS SoC, although these two ESS types involve different dynamics.

With respect to the short duration and high power density, probably the most demanding AS is the virtual inertia. Some previous works consider unlimited energy and an infinite DC bus, thus just paying attention on the CIRES control required for the AS provision [13]–[15]. With this regard, the DC-link dynamics are neglected when the virtual inertia is provided. There are some research efforts, however, which include an ESS to provide the required amount of virtual inertia. In [16] virtual inertia is provided by a FW but its recovery after the AS provision is not studied. The BESS SoC restoration after the virtual inertia provision is analyzed in [17], [18], which is characterized by a slower dynamics due to its inherent larger time constant. With this regard, FESS are preferred for this type of AS with short time duration and high power density. However, an adequate SoC recovery strategy after the AS provision has not been properly addressed in the specialized literature.

This paper comes to fill this gap by proposing a new control strategy for the SoC recovery after the virtual inertia provision by a CIRES involving a FESS. With the proposed control strategy, the following two main objectives are achieved:

- Fast and precise FESS energy control to recover the steady-state conditions after an AS provision.
- Precise energy release required for bringing the inertial response.

The main advantage of the proposed control strategy is that the both objectives can be achieved at the same time if the FESS operation is within their technical operational limits. If this is not the case, i.e. operation outside of the safe working area, the controller prioritizes the SoC recovery to its steady-state reference value.

II. MODEL DEFINITION

The aim of this section is to define the dynamic model used in the proposed FESS control algorithm. Fig. 1 depicts the system under study which is composed of a CIRES with a FESS. The power magnitudes used in the system modelling and the control algorithm are also summarized in Tab. I.

Regarding the CIRES, it is proposed to control it as a Virtual Synchronous Generator (VSG) in order to provide virtual inertia. With this regard, any of the control schemes already proposed in the literature can be applied [13]–[15]. Any of

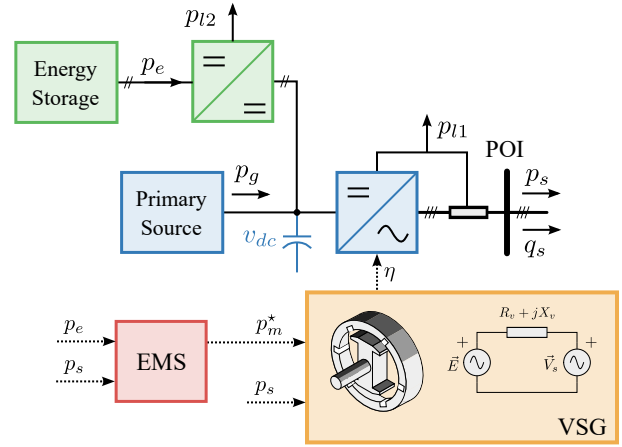


Fig. 1. System under study composed of a CIRES with a FESS and corresponding power magnitudes used in the model and control algorithm.

TABLE I
VARIABLES USED IN THE PROPOSED CONTROL ALGORITHM.

POI	Point Of Interconnection.
p_s	POI active power (p.u.).
q_s	POI reactive power (p.u.).
p_g	Primary source power (p.u.).
p_e	FESS power (p.u.).
p_{l1}	VSC energy losses (p.u.).
p_{l2}	DC/DC converter energy losses (p.u.).
p_l	Actual total losses (p.u.).
\hat{p}_l	Estimated total losses (p.u.).
p_r	Restoring power (p.u.).
x	Storage main state (i.e. speed for FW or voltage for SC)
E_0	Desired steady-state storage energy (J).
E	Actual storage energy (J).
ΔE^*	FESS estimated energy increment (J).
ΔE_r	FESS estimated restoration energy increment (J).

these available methods is based on the virtual mechanical power which can be defined as:

$$p_m^* = p_g + \hat{p}_l + p_e^*(E, E^*), \quad (1)$$

where p_g is the measured power of the primary energy source, \hat{p}_l is an estimation of the system losses, p_e^* is the FESS reference power which will depend on the reference FESS energy E^* as explained in the next section. Note that the system losses are those of the VSC and DC/DC converter interfacing the FESS and can be computed applying a simple power balance as:

$$\hat{p}_l = p_{l1} + p_{l2} = p_e + p_g - p_s \quad (2)$$

On the other hand, the FESS dynamics can be modelled as the nonlinear first order differential equation as a function of the FESS power p_e used to charge or discharge it:

$$\frac{dx}{dt} = -\frac{p_e}{xM}, \quad (3)$$

where x is the main state to control and M is the FESS time constant (i.e. speed and moment of inertia in a FW or voltage

and capacitance in case the of a SC). Obviously, this model is just an approximation and neglects other dynamics and FESS power losses but it is sufficient for the proposed controller development. The FESS stored energy is defined as:

$$E = \frac{1}{2} Mx^2 = \int p_e dt. \quad (4)$$

III. CONTROL STRATEGY

This section outlines the control scheme for the FESS Energy Management System (EMS) in order to fulfil the aforementioned objectives. The FESS-EMS, denoted with the red rectangle in Fig. 1 is detailed in Fig. 2. Basically, this FESS-EMS is composed of two main control blocks which are devoted to compute an adequate FESS reference power p_e^* to provide the virtual inertia provision as close as possible to the theoretical one but considering also an optimal SoC recovery after any event. Note that these two objectives are totally opposite as the virtual inertia response leads to an energy release and, therefore, a SoC deviation from the reference value. For this reason, any SoC recovery strategy based on conventional droop controllers to maintain the SoC to a reference value poses some drawbacks depending on the applied controller gains. Large control gains will recover the SoC to the reference value quite fast but a cost of affecting the provided virtual inertia. On the contrary, small droops may not interfere the AS provision but a quite large SoC restoration time is expected.

To overcome this shortcoming, the first control block of the proposed strategy is based on a variable droop controller where the reference FESS energy is constantly modified according to an estimation of the FESS energy release which is used as an indicator of the AS provision. In addition, the second control block computes a power term which is used for SoC recovering purposes. The following subsections are devoted to give the details of each of these control blocks.

A. Energy release control block

The energy release control block is based on a droop curve shown in Fig. 3 which defines the reference FESS power p_e^* as a function of a variable reference energy E^* . Note that those points of the curve related to the FESS operational limits do not vary: (p_e^{max}, E_{min}) and (p_e^{min}, E_{max}) . These maximum and minimum energies are computed with (4) using the state variable limits x_{min} and x_{max} . On the contrary, the other points of the droop curve are modified according to the deviation of the reference FESS energy, E^* , with respect to its reference value $E_0 = \frac{1}{2}(E_{max} + E_{min})$:

$$\Delta E^* = E^* - E_0 \quad (5)$$

This reference FESS energy, E^* , is just the estimation of the FESS delivered energy, \hat{E} , bounded within the FESS operational limits within E_{min} and E_{max} as shown in Fig. 2. The estimation of the FESS energy release, \hat{E} , depends on the estimation of the power required to provide the virtual

TABLE II
CONSIDERED PARAMETERS FOR THE SIMULATIONS.

Main VSC nominal power = 20 kVA
FESS type: Ultracapacitor
C 5 F
V_{min} 80 V $\Rightarrow E_{min}=64$ kJ
V_{max} 160 V $\Rightarrow E_{min}=256$ kJ
V_0 126.49 V $\Rightarrow E_{min}=160$ kJ

inertia, \hat{p}_e , and the power required to restore the SoC value, p_r , which is analyzed in the next subsection:

$$\frac{d\Delta\hat{E}}{dt} = -\hat{p}_e + p_r. \quad (6)$$

Finally, note that \hat{p}_e can be computed using the definition of the virtual mechanical power as:

$$\hat{p}_e = p_h = p_s - p_m^* \quad (7)$$

where p_h is the inertial response power.

B. Energy recovery control block

The power term p_r responsible for the SoC recovery is defined as:

$$p_r = \begin{cases} p_r^*, & \text{if } \Delta E^* < 0 \wedge \Delta E^* < \Delta E_r \\ -p_r^*, & \text{if } \Delta E^* > 0 \wedge \Delta E^* > \Delta E_r \\ 0, & \text{if } |E^* - E_0| < \text{tol.} \end{cases} \quad (8)$$

where p_r^* is a constant and predefined power, ΔE^* is calculated with (5) and ΔE_r is the virtual recovery energy deviation with respect E_0 . This new virtual variable follows the dynamics:

$$\frac{d\Delta E_r}{dt} = -K_m \hat{p}_e + p_r - K_r \Delta E_r \quad (9)$$

where K_m and K_r are parameters to be defined. Note that $K_m > 1$ in order to guarantee that ΔE_r is larger than $\Delta\hat{E}$. Once K_m is chosen, K_r can be defined to adjust the time constant of this first-order system (e.g. how fast the energy starts to recover). The virtual recovery energy can be computed as:

$$E_r = \Delta E_r + E_0. \quad (10)$$

IV. SIMULATION RESULTS

Simulations have been performed using a specific open-source software written in python called PyDAE which is publicly available in [19]. This software is specially suited to solve efficiently a set of Differential-Algebraic Equations (DAE). For this purpose, the DAE corresponding to the system shown in Fig. 1 is derived. Basically, this system is composed of a three phase dc/ac converter with its coupling filter, a dc/dc converter interfacing the FESS with the common DC bus and a primary energy source. The main parameters of the system are shown in Tab. II.

The next subsections are devoted to show the performance of the proposed control algorithm. Particularly, two inertia

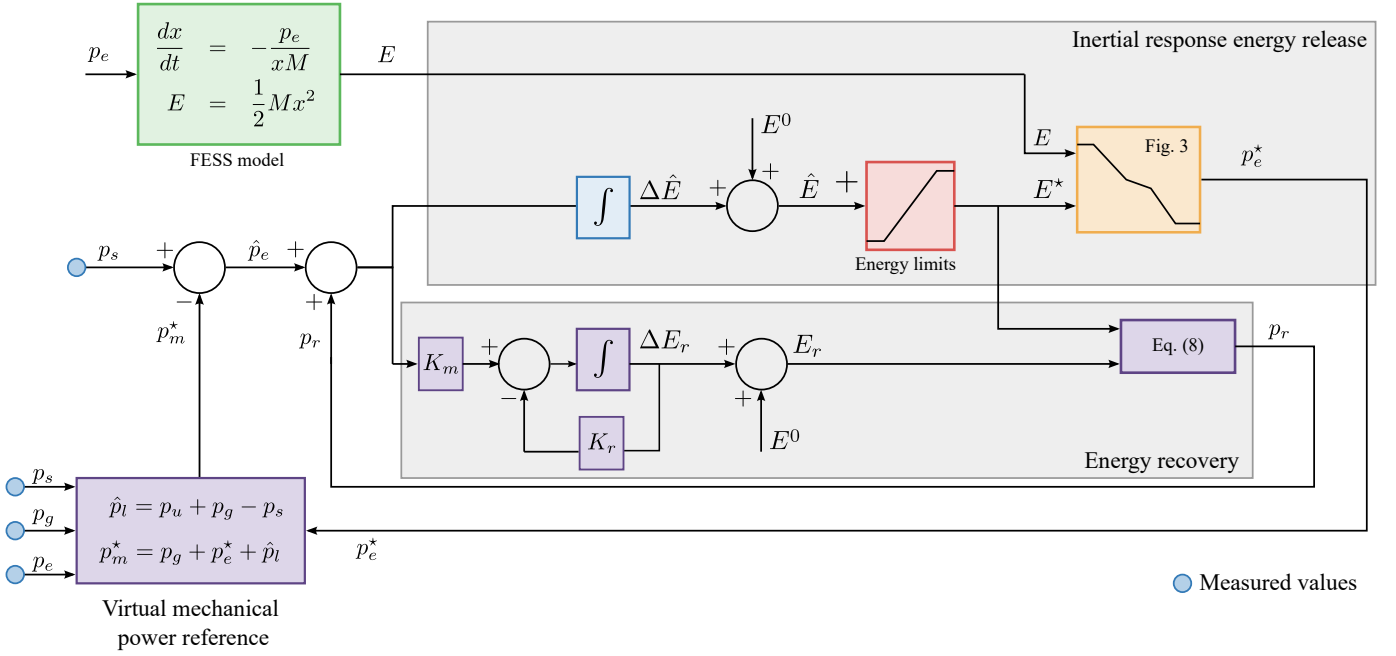


Fig. 2. Proposed FESS controller.

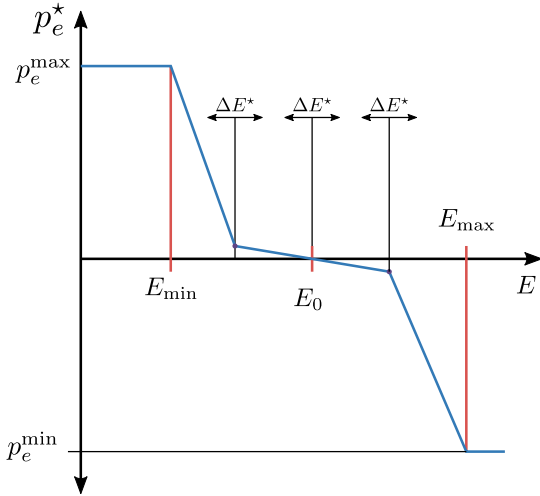


Fig. 3. Energy-Power Droop.

provision scenarios are simulated with different energy requirements. In the first case, the AS is provided without reaching any operational SC limit. Conversely, the second scenario is devoted to highlight the controller performance when the predefined energy threshold is reached. Finally, the proposed algorithm is compared to a classical droop approach to evidence its improved performance.

A. Moderate inertial response

The first test consists of a moderate inertial response where the FESS energy limits are not reached and the desirable inertia constant is $H = 7s$. The power system frequency changes from 50 Hz to 47 Hz in 5 seconds (RoCoF of -0.5

Hz/s) as shown in the top plot of Fig. 4. The middle plot shows the actual FESS energy E blue, its reference value E^* and the virtual recovery energy E_r with green and yellow colours respectively. As it can be observed in the bottom plot of Fig. 4, the obtained power p_s follows the desired value p_s^* during the frequency ramp variation that can be computed as:

$$\Delta p = 2H RoCoF p^u = 2 \times 7s \frac{0.5 Hz/s}{50 Hz} = 0.14 pu, \quad (11)$$

When the frequency reaches the new steady state, the FESS energy remains constant until E_r becomes larger than E^* and the recovery power p_r starts charging the FESS. Note that the recovery control logic defined by (8) naturally introduces a dead time after the inertia provision which is controlled by the parameter K_r . This performance is suitable from the power system point of view because after the frequency event, produced due to an imbalance between generation and demand, the FESS energy restoration is delayed contributing somehow to reduce further frequency variations.

B. Inertial response with energy saturation

The second test is similar to the first one, but considering a larger $RoCoF = 1 Hz/s$. This event has associated a larger energy release which activates the FESS lower energy limit E_{min} . The simulation results are shown in Fig. 5 in green colour along with the previous simulation with $RoCoF = 0.5 Hz/s$ in red colour comparison purposes. The bottom plot of the figure clearly evidences that the power follows the increment Δp defined in (11) for $RoCoF = 1 Hz/s$ until the lower energy threshold E_{min} is reached in spite of the frequency still is decreasing. After the event, the proposed algorithm makes the inertial response null as expected. Regarding the delivered

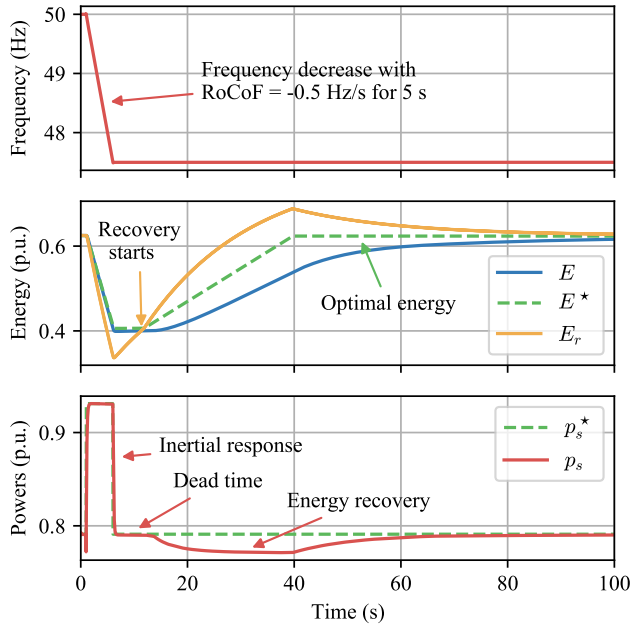


Fig. 4. Frequency, energies evolution and power during moderate inertial response.

FESS energy, the middle plot shows the evolution of E^* and E with dash and continuous lines respectively.

C. Comparative with conventional approach

Finally, the proposed method is compared with the conventional Proportional-Integral (PI) controller for the FESS energy restoration. More specifically, this PI controller is supposed to exist in the red box named EMS within Fig. 1 and will be defined by the following control law,

$$p_e^* = K_p (E_0 - E) + K_i \int (E_0 - E) dt \quad (12)$$

Two cases are considered for the PI: high gain and low gain. In this paper, $K_p = 0.01$ and $K_p = 0.045$ are considered and $K_i = K_p/T$, where $T = 60s$. As it can be seen in Fig. 6, the low gain PI (red curve) gives an inertial response that is close to the ideal one, but the energy recovery can take around five minutes. In the other hand, a PI with a high gain (green curve) that gives the same recovery time to current proposal but with an inertial response that is far from the desired one.

V. CONCLUSIONS

In this paper, a novel energy recovery scheme for fast acting energy storage systems (FESS) connected to converter-interfaced RES (CIRES) is proposed, when the CIRES is assumed to provide Ancillary Services (AS). FESS, like SCs or FWs, are the most appropriate ESS to assist the CIRES with short-duration high power-demanding AS, like virtual inertia provision or high frequency power smoothing. For this reason, in this study the new controller is tested during abrupt frequency variations with moderate and high values of Rate

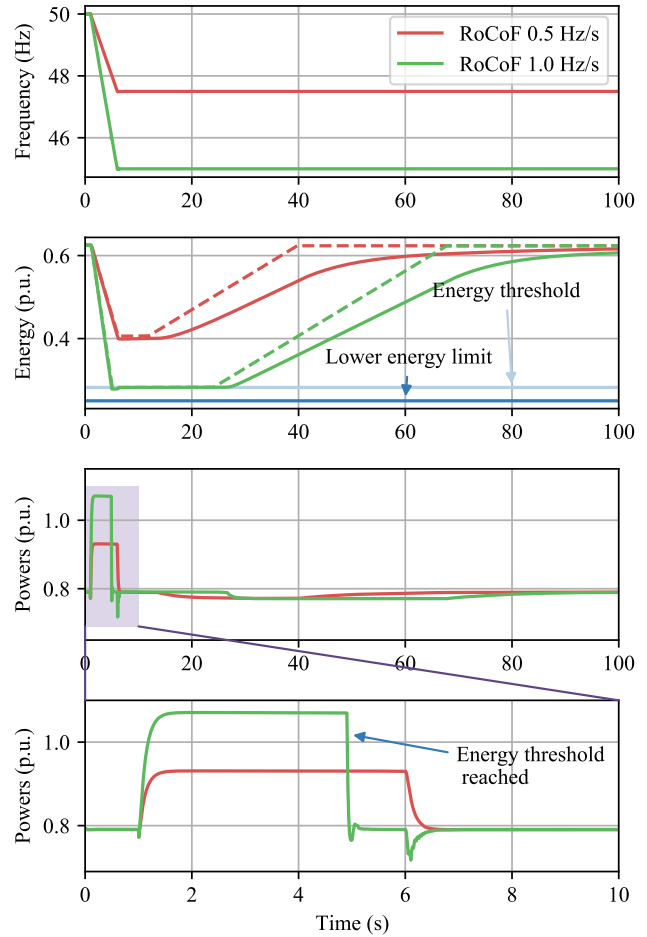


Fig. 5. Inertial responses with and without lower energy saturation.

of Change of Frequency (RoCoFs), so that its performance is evidenced by the achieved virtual inertia provision and the quick recovery of the FESS. Finally, the performance of the proposed controller is tested against an energy recovery scheme implemented by a simple PI controller with high and low gains, stressing out the drawbacks of such simplistic solutions in the energy recovery schemes of FESS.

REFERENCES

- [1] C. S. Demoulias, K.-N. D. Malamaki, S. Gkavanoudis, J. M. Mauricio, G. C. Kryonidis, K. O. Oureilidis, E. O. Kontis, and J. L. Martinez Ramos, "Ancillary services offered by distributed renewable energy sources at the distribution grid level: An attempt at proper definition and quantification," *Applied Sciences*, vol. 10, no. 20, 2020.
- [2] R. van Haaren, M. Morjaria, and V. Fthenakis, "An energy storage algorithm for ramp rate control of utility scale pv (photovoltaics) plants," *Energy*, vol. 91, pp. 894 – 902, 2015.
- [3] M. E. Amiryar and K. R. Pullen, "A review of flywheel energy storage system technologies and their applications," *Applied Sciences*, vol. 7, no. 3, 2017.
- [4] M. Ceraolo, G. Lutzemberger, and D. Poli, "State-of-charge evaluation of supercapacitors," *Journal of Energy Storage*, vol. 11, pp. 211–218, 2017.
- [5] J. W. Shim, G. Verbič, H. Kim, and K. Hur, "On droop control of energy-constrained battery energy storage systems for grid frequency regulation," *IEEE Access*, vol. 7, pp. 166353–166364, 2019.

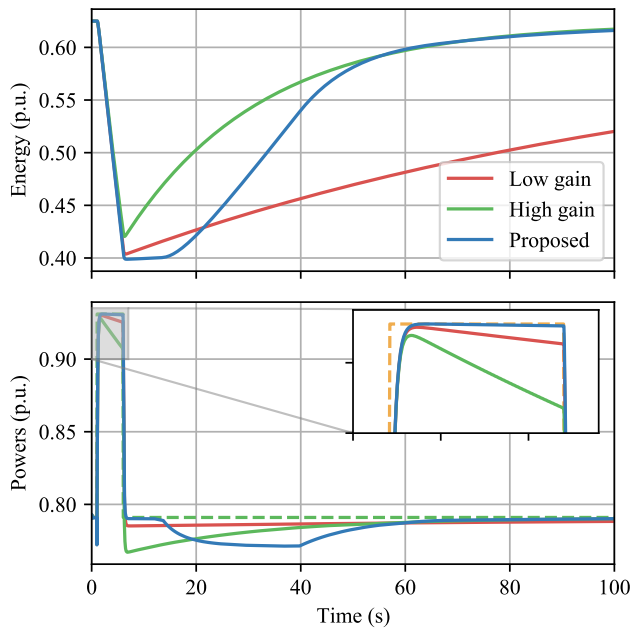


Fig. 6. PI control with high and low gain and proposed strategy

- [6] D. Mejía-Giraldo, G. Velásquez-Gomez, N. Muñoz-Galeano, J. B. Cano-Quintero, and S. Lemos-Cano, "A bess sizing strategy for primary frequency regulation support of solar photovoltaic plants," *Energies*, vol. 12, no. 2, 2019.
- [7] J. Cao, W. Du, H. Wang, and M. McCulloch, "Optimal sizing and control strategies for hybrid storage system as limited by grid frequency deviations," *IEEE Transactions on Power Systems*, vol. 33, no. 5, pp. 5486–5495, 2018.
- [8] Q. Yan, Q. Bo, Y. Jingjie, M. Yunfei, and G. Bingqing, "Frequency control strategy of hybrid energy storage system for microgrid based on frequency hysteretic loop," *Energy Procedia*, vol. 103, pp. 328 – 332, 2016. *Renewable Energy Integration with Mini/Microgrid – Proceedings of REM2016*.
- [9] Y. Yuan, C. Sun, M. Li, S. S. Choi, and Q. Li, "Determination of optimal supercapacitor-lead-acid battery energy storage capacity for smoothing wind power using empirical mode decomposition and neural network," *Electric Power Systems Research*, vol. 127, pp. 323 – 331, 2015.
- [10] M. J. E. Alam, K. M. Muttaqi, and D. Sutanto, "A novel approach for ramp-rate control of solar pv using energy storage to mitigate output fluctuations caused by cloud passing," *IEEE Transactions on Energy Conversion*, vol. 29, no. 2, pp. 507–518, 2014.
- [11] P. Zhao, J. Wang, and Y. Dai, "Capacity allocation of a hybrid energy storage system for power system peak shaving at high wind power penetration level," *Renewable Energy*, vol. 75, pp. 541 – 549, Mar. 2015.
- [12] L. Barelli, G. Bidini, D. Pelosi, D. Ciupageanu, E. Cardelli, S. Castellini, and G. Lăzăroiu, "Comparative analysis of ac and dc bus configurations for flywheel-battery hess integration in residential micro-grids," *Energy*, vol. 204, p. 117939, 2020.
- [13] T. Qoria, E. Rokrok, A. Bruyere, B. François, and X. Guillaud, "A pll-free grid-forming control with decoupled functionalities for high-power transmission system applications," *IEEE Access*, vol. 8, pp. 197363–197378, 2020.
- [14] V. Natarajan and G. Weiss, "Synchronverters with better stability due to virtual inductors, virtual capacitors, and anti-windup," *IEEE Transactions on Industrial Electronics*, vol. 64, no. 7, pp. 5994–6004, 2017.
- [15] S. Tan, H. Geng, and G. Yang, "Modeling framework of voltage-source converters based on equivalence with synchronous generator," *J. Mod. Power Syst. Clean Energy*, vol. 6, p. 1291–1305, 2018.
- [16] J. Yu, J. Fang, and Y. Tang, "Inertia emulation by flywheel energy storage system for improved frequency regulation," in *2018 IEEE 4th Southern Power Electronics Conference (SPEC)*, pp. 1–8, 2018.
- [17] H. Golpira, A. Atarodi, S. Amini, A. R. Messina, B. Francois, and H. Bevrani, "Optimal energy storage system-based virtual inertia placement: A frequency stability point of view," *IEEE Transactions on Power Systems*, vol. 35, no. 6, pp. 4824–4835, 2020.
- [18] U. Datta, A. Kalam, and J. Shi, "Battery energy storage system for aggregated inertia-droop control and a novel frequency dependent state-of-charge recovery," *Energies*, vol. 13, no. 8, 2020.
- [19] J. M. Mauricio, "Pydae." <https://github.com/pydae/pydae>, 2020.